Paleobiology, 41(3), 2015, pp. 460–478
DOI: 10.1017/pab.2015.11

Using experimental decay of modern forms to reconstruct the early evolution and morphology of fossil enteropneusts

Karma Nanglu, Jean-Bernard Caron, and Christopher B. Cameron

Abstract.—Decay experiments are becoming a more widespread tool in evaluating the fidelity of the fossil record. Character interpretations of fossil specimens stand to benefit from an understanding of how decay can result in changes in morphology and, potentially, total character loss. We performed a decay experiment for the Class Enteropneusta to test the validity of anatomical interpretations of the Burgess Shale enteropneust *Spartobranchus tenuis* and to determine how the preservation of morphological features compares with the sequence of character decay in extant analogues. We used three species of enteropneust (*Saccoglossus pusillus*, *Harrimania planktophilus*, and *Balanoglossus occidentalis*) representing the two major families of Enteropneusta. Comparisons between decay sequences suggest that morphological characters decay in a consistent and predictable manner within Enteropneusta, and do not support the hypothesis of stemward slippage. The gill bars and nuchal skeleton were the most decay resistant, whereas the gill pores and pre-oral ciliary organ were unequivocally the most decay prone. Decay patterns support the identification of the nuchal skeleton, gill bars, esophageal organ, trunk, and proboscis in *Spartobranchus tenuis* and corroborate a harrimaniid affinity. Bias due to the taphonomic loss of taxonomically informative characters is unlikely. The morphologically simple harrimaniid body plan can be seen, therefore, to be plesiomorphic within the enteropneusts. Discrepancies between the sequence of decay in a laboratory setting and fossil preservation also exist. These discrepancies are highlighted not to discredit the use of modern decay studies but rather to underline their non-actualistic nature. Paleoenvironmental variables besides decay, such as the timeframe between death and early diagenesis as well as postmortem transport, are discussed relative to decay data. These experiments reinforce the strength of a comprehensive understanding of decay sequences as a benchmark against which to describe fossil taxa and understand the conditions leading to fossilization.

Karma Nanglu. Department of Ecology and Evolutionary Biology, University of Toronto, Toronto, Ontario M5S 2J7, Canada, and Department of Natural History Palaeobiology, Royal Ontario Museum, Toronto, Ontario M5S 2C6, Canada. E-mail: karma.nanglu@alum.utoronto.ca
Jean-Bernard Caron. Department of Natural History Palaeobiology, Royal Ontario Museum, Toronto, Ontario M5S 2C6, Canada. Departments of Ecology and Evolutionary Biology and Earth Sciences, University of Toronto, Toronto, Ontario M5S 2J7, Canada
Christopher B. Cameron. Département de sciences biologiques, Université de Montréal C.P. 6128, Succursale Centre-ville, Montreal, Quebec H3C 3J7, Canada

Accepted: 17 December 2014

Introduction

The differential loss of morphological characters due to postmortem decay, hereafter "decay bias," presents a potentially significant impediment to the interpretation of fossils, especially those of soft-bodied organisms preserved in various fossil Lagerstätten. With the onset of decay, taxonomically informative features can be lost or altered. Estimating the amount of decay bias is therefore of particular significance when considering, for example, problematic Cambrian soft-bodied fossils for which multiple disparate interpretations have been offered (e.g., Yunnanozoon [Chen et al. 1995; Shu et al. 1996; Chen and Huang 2008]; for a review of several case studies, see Donoghue and Purnell 2009). Delineating taphonomic loss from true phylogenetic absence remains a central question in paleontology and this question has received renewed interest in recent years, especially since the introduction of the "stemward slippage" concept (Sansom et al. 2010a,b). This concept is based on the theory that taxa are placed erroneously basal due to the underlying bias of many synapomorphic characters to early decay over plesiomorphic ones. However, it remains to be seen if stemward slippage is ubiquitous among animal groups beyond vertebrates (Sansom and Wills 2014).

 0094-8373/15

Decay experiments potentially provide a useful tool to estimate taphonomic biases. Such experiments have been used to investigate a number of factors, including the role of anoxia in the preservation of soft-bodied organisms (Allison 1986), the relative contribution of transport in fossil articulation and completeness (Allison 1988), the degree to which decay alters soft tissues (Briggs and Kear 1993a) and how such data can be useful to infer taphonomy at the community level (Briggs and Kear 1993b; Caron and Jackson 2006). Decay experiments are also used to infer the physical and chemical composition of extinct taxa and the potential chemical and geologic pathways of preservation (Briggs and Kear 1994; Briggs et al. 1995), including effects of sediment type on rate of decomposition (Wilson and Butterfield 2013) and the preservation-enhancing potential of microbial death masks on organic material (Darroch et al. 2012). Quantifying the cumulative rate of decay of morphological characters over time (Casenove et al. 2011), and creating cross-comparisons of decay sequences among phylogenetically important extant proxies to serve as a visual guide for fossil interpretation (Sansom et al. 2013) have also stemmed from experimental decay studies. However, the usefulness of such studies has also been called into question when they are used without a critical reappraisal of the fossil record, including direct and extensive comparisons of data from decay experiments with fossils (Conway Morris and Caron 2012).

Here, we present the experimentally derived taphonomy and sequence of decay and decomposition of three enteropneust (acorn worm) species from two phylogenetically distant families (Fig. 1). This research is the most extensive comparison of decay sequences of a single fossil taxon and the first of its kind for acorn worms. The Hemichordata, including

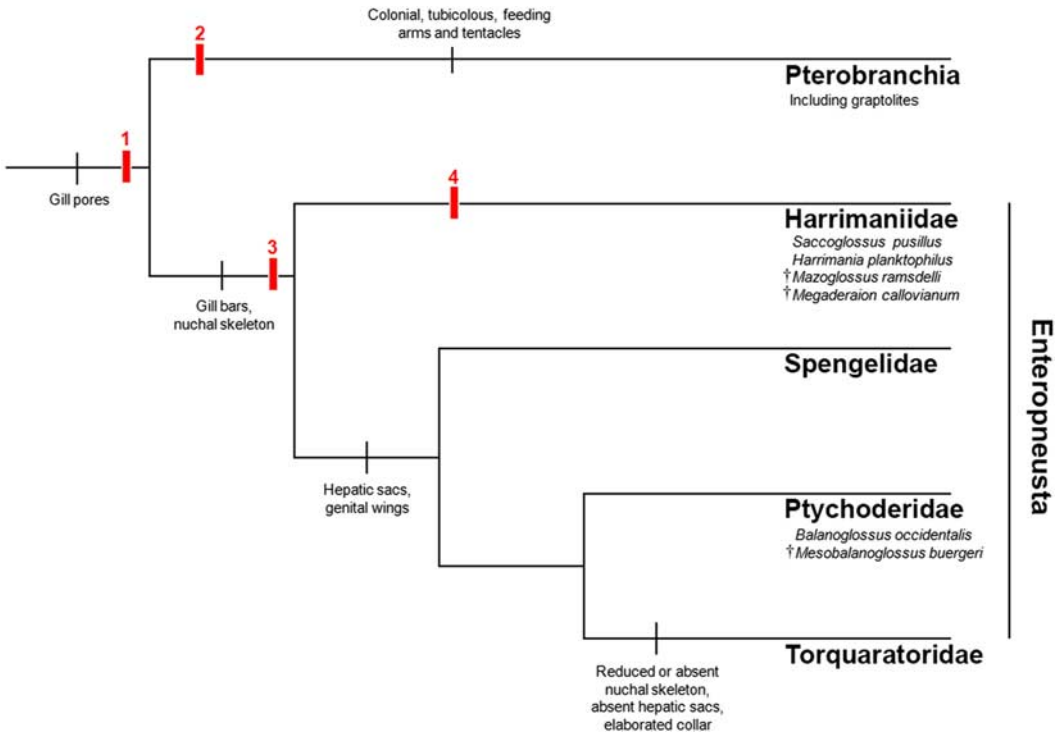

FIGURE 1. Phylogenetic tree of the hemichordates. The pterobranch *Cephalodiscus* has a single pair of gill pores, whereas gill slits with a collagenous skeleton are an enteropneust (and chordate) feature. Among the enteropneusts, genital wings and hepatic sacs are found in ptychoderids and some spengelids, but not harrimaniids. The nuchal skeleton is reduced or absent from the deep-sea torquaratorids. Red numbered bars indicate potential hypotheses for the phylogenetic position of *Spartobranchus tenuis*: 1, stem hemichordate; 2, stem pterobranch; 3, stem enteropneust; 4, stem harrimaniid (Caron et al. 2013).

https://doi.org/10.1017/pab.2015.11 Published online by Cambridge University Press

the class Enteropneusta, are sister to the Echinodermata, with which they form the superphylum Ambulacraria. Ambulacrarians are sister taxa to the Chordates and together constitute the deuterostome branch of animal life (Cameron 2005). While these inter-phylum relationships are strongly supported, the phylogeny within the hemichordates has been a matter of historical debate. Much of this debate centers on the relationship between the two hemichordate classes, which are morphologically disparate: the Enteropneusta are solitary and vermiform, whereas the Pterobranchia are colonial and tube-dwelling. The pterobranchs, primarily the graptolites, are abundant in the fossil record owing to the robustness of their tubaria, and have important implications for dating rock sequences (Mitchell et al. 2013; Maletz 2014).

In contrast, findings of putative enteropneusts in the fossil record have been rare (Arduini et al. 1981; Bechly and Frickhinger 1999; Alessandrello et al. 2004), taxonomically contentious (Szaniawski 2005; Conway Morris 2009; Szaniawski 2009), and descriptively uninformative (Shabica and Hay 1997). First described in 1911 from the Burgess Shale, Yoho National Park, *Spartobranchus tenuis* was recently redescribed as an enteropneust living in tubes and most resembling the extant family Harrimaniidae (Caron et al. 2013; but see Halanych et al. 2013 and Cannon et al. 2013 for an alternative hypothesis). Three factors make *S. tenuis* critical to understanding the origin and early evolution of hemichordates. First, its exceptional quality of preservation reveals more aspects of the internal anatomy than any other fossil enteropneust. Second, its Cambrian origins push back the earliest known instance of enteropneusts in the fossil record approximately 200 Myr (the previous earliest known fossil enteropneusts are Pennnsylvanian). Third, thousands of specimens allow us to make robust cross-comparisons of anatomical features and correctly identify anomalous characters that may be artifacts of decay/preservation. Furthermore, the broad morphological similarity of modern taxa to *S. tenuis* means that acorn worms are ideal candidates for an experimental decay study; it is possible to directly compare their anatomies without having to observe decay in a range of extant species to account for different possible morphological aspects of the ancestral form (Sansom et al. 2013). These factors, when considered alongside the hypothesis that the ancestral deuterostome body plan may have resembled that of an acorn worm (Cameron et al. 2000), underline the need for a comprehensive understanding of the early evolutionary history of the hemichordates (Swalla and Smith 2008). The goals of our experiment were therefore to: (1) describe the sequence and rate of morphological character decay of the Enteropneusta, (2) perform direct and exhaustive comparisons with the anatomy of the fossil enteropneust *S. tenuis*, (3) consider the phylogenetic position of *S. tenuis* and implications on the early evolution of the Enteropneusta and interrelationships within Hemichordata, (4) analyze the strengths and weaknesses of decay experiments for describing fossil anatomy, and (5) use our understanding of enteropneust decay to make inferences regarding the taphonomic setting of the Burgess Shale.

Materials and Methods

Saccoglossus pusillus and *Harrimania planktophilus* ($n = 60$ and 34, respectively) were collected by K.N. and C.B.C. in the Cape Beale Inlet, British Columbia, Canada, in May and June 2013, using a shovel and hand sieve. Specimens were immediately transported to the nearby Bamfield Marine Sciences Centre and were kept alive with continuous circulating seawater for a maximum of two weeks prior to euthanasia. *Balanoglossus occidentalis* ($n = 12$) were collected by CBC in July 2013 from Penrose Point State Park, Washington, U.S.A., and shipped in seawater on ice to the Royal Ontario Museum in Toronto. Because of the limited number of specimens available and the frequency of breakage of *B. occidentalis* specimens during extraction, experiments were conducted on fragmented as well as whole individuals. All damage occurred posterior to the pharyngeal trunk; pharyngeal fragments were placed with corresponding trunk fragments during the experiment. Only completely undamaged specimens of *S. pusillus* and *H. planktophilus* were used.

https://doi.org/10.1017/pab.2015.11 Published online by Cambridge University Press

All specimens were euthanized following previous protocols (Cameron 2002), with a prolonged exposure to a 50:50 solution of magnesium chloride ($MgCl_2$, 75 mg/ml) and artificial seawater (Instant Ocean brand artificial seawater, specific gravity = 1.02). In enteropneusts, determining time of death, and therefore the theoretical beginning of decay, is difficult. In the absence of a brain, or any true centralized nervous system, "death" can be an ambiguous term. For the purpose of this study, we defined death as the moment that physical stimulation ceased to elicit muscle contractions. This state occurred within approximately 30 minutes of exposure to $MgCl_2$. Specimens were not sterilized or chemically treated in any way prior to the experiment and were kept alive in continuously circulating seawater for any time spent in the laboratory prior to euthanasia. Microbes involved in postmortem decay, therefore, would have consisted of those already found in the gut contents of the specimens as well as on the ectoderm.

The decay experiment methodology generally followed that of Sansom et al. 2010a on chordate decay, but with some modifications: after 30 minutes of exposure to the $MgCl_2$ and artificial seawater mixture, specimens were placed in individual Petri dishes filled with the same solution. Specimens were placed into a trough made by bisecting a plastic straw down its length. The purpose of the straw was twofold. First, it prevented postmortem movement of the worm during transport into and out of the incubator. Second, it helped to keep the remains intact and generally contiguous during the decay process, thus mimicking the potential effects of being entombed in mud layers. To limit gas exchange and create conditions leading to dysoxia, Petri dishes were sealed with Parafilm immediately prior to incubation. Specimens were incubated at 17°C for the following number of days: *S. pusillus*, ten days, *H. planktophilus*, five days, and *B. occidentalis*, eight days.

Characters scored for their decay rates are described in Figure 2 and Table 1. Decay gradients were evaluated on a scale of 1 to 5, with the following definitions: (1) pristine characters showing no signs of decay, (2) superficial decay, such as wrinkling or fraying, (3) significant wrinkling and fraying and/or loss of structural rigidity, (4) advanced decay but with characters still recognizable, and (5) characters unrecognizable or completely disintegrated. Observation intervals were chosen based on pre-experimental trials (every 12 hours for *S. pusillus*, every 6 hours for *H. planktophilus*, at 48 hours, 72 hours, 96 hours, and 168 hours for *B. occidentalis*), which determined the total time required for a specimen to progress from pristine to completely disintegrated—up to ten days in the case of *S. pusillus*—with the exception of the gill bars and nuchal skeleton, which remained intact for the duration of the experiment. At each interval, three *S. pusillus*, two *H. planktophilus*, and two *B. occidentalis* were removed from the incubator and observed under a stereomicroscope. The outer morphology was observed first, before specimens were dissected for observation of the internal organs. Each morphological character of interest was scored according to the predetermined decay gradient scale.

We compared specimens of *S. tenuis* from the Royal Ontario Museum and the Smithsonian National Museum of Natural History with the results of the experiments in order to describe their anatomy with reference to extant Enteropneust morphology and the observed sequence of character decay.

Results

Figure 3 shows the sequence of character decay for *S. pusillus*, *H. planktophilus*, and *B. occidentalis*. The decay of enteropneust characters was broadly grouped into four stages (Figs. 4, 5). The time it took to enter and pass through each stage varied according to species, but each stage was descriptive of the level of decay of each character of interest relative to other characters. Table 1 summarizes the sequence of decay for each character. Among all species, the gill pores and pre-oral ciliary organ were the first characters to decay. The longitudinal proboscis muscles showed signs of early decay (lack of clear definition of the concentric rings of muscle bands), but were

https://doi.org/10.1017/pab.2015.11 Published online by Cambridge University Press

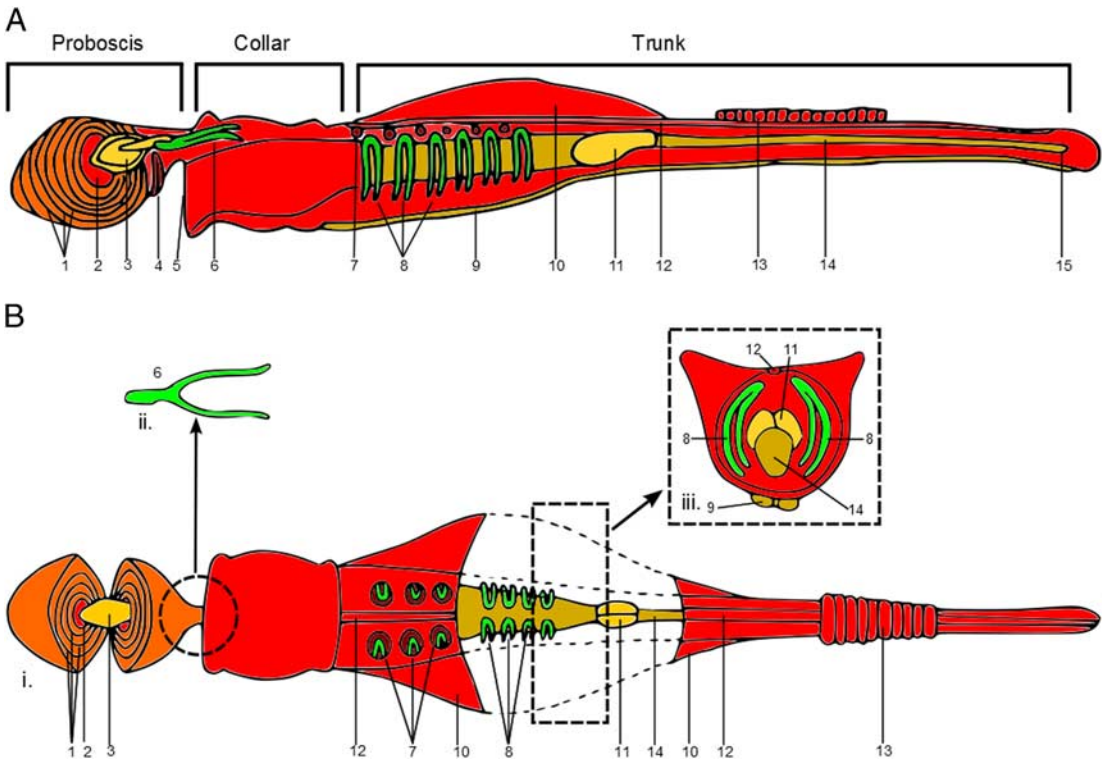

FIGURE 2. A, Generalized anatomy of the Enteropneusta (lateral view) and sequence of decay of major features. The division of tripartite body plan (proboscis, collar, trunk) is highlighted. Susceptibility of decay proceeds from dark red (gill pores and pre-oral ciliary organ) to light red, yellow, orange, light green, dark green (gill bars and nuchal skeleton). 1, Longitudinal proboscis muscles. 2, Proboscis coelomic cavity. 3, Heart-kidney-stomochord complex. 4, Pre-oral ciliary organ. 5, Mouth. 6, Nuchal skeleton. 7, Gill pores. 8, Gill bars. 9, Ventral midline. 10, Genital wings. 11, Esophageal organ. 12, Dorsal midline. 13, Hepatic sacs. 14, Digestive tube (genital wings and hepatic sacs are absent from Harrimaniidae). 15, Anus. B (i) Dorsal view; (ii) Dorsal view of the nuchal skeleton displaying characteristic "Y" shape (found internally and beneath the stomochord in the dashed-circled region); (iii) cross-section of the dashed-boxed region; gill bars curve laterally around the columnar trunk.

recognizable in a highly decayed form until the late stages of the experiment. Among all species, the gill bars and nuchal skeleton were the most decay resistant.

During stage 1, the specimen appeared nearly pristine externally. The ectoderm had begun to fray, but was generally contiguous and resistant to tearing. The gill pores were not identifiable by the end of stage 1, but most internal organs remained in a pristine state of preservation comparable to those of freshly euthanized specimens. The most significant damage was generally in the posterior or intestinal trunk, i.e., posterior to the pharyngeal trunk. Ruptures may have formed in the trunk ectoderm, although the location of any given rupture along the trunk was variable. Gut contents were sometimes seen spilling into the surrounding environment, indicating that, in some specimens, the intestinal endoderm had also ruptured.

In stage 2, the specimen was intact but was clearly undergoing decay. The ectoderm had lost elasticity, and presented very little resistance to forceps. The proboscis coelom had collapsed and the longitudinal proboscis muscles had liquefied. These factors together presented a proboscis with little to no rigid structure. In the pharynx, the collagenous nuchal skeleton and gill bars remained undamaged and undisturbed topographically. The heart-kidney-stomochord complex had lost definition and was beginning to dissolve into the surrounding medium. In the trunk, damage that occurred during stage 1 continued to progress. Sections of the trunk may have become detached from one another, or

https://doi.org/10.1017/pab.2015.11 Published online by Cambridge University Press

TABLE 1. Morphological characters of enteropneusts involved in the decay experiment (number in brackets indicates corresponding position in Fig. 2). Stages of decay are illustrated in Figures 4 and 5.

Character	Description	Pattern of decay
Proboscis	The anterior soma or segment of the enteropneust that, when pulled up against the collar soma, often results in an acorn shape, hence the common name "acorn worm."	• Consistently show early decay: fraying of the ectoderm and loss of external definition. • Occasionally rupture, usually at anterior most point. • Total disintegration usually did not occur until late stage 3 due to some tissue remaining intact at the anterior nuchal skeletal region.
Longitudinal proboscis muscles (1)	Arranged diffusely in *Harrimania*, in concentric rings in *Saccoglossus* and as radial plates in *Balanoglossus* (see Deland et al. 2010).	• Decay begins as loss of muscle definition. • Could remain present at later stages of decay as undefined masses of liquefied tissue.
Proboscis coelomic cavity (2)	Fluid filled cavity of variable size that contains the heart-kidney-stomochord complex.	• Early loss of fluid and deflation from a characteristic round structure by the end of stage 1 to early stage 2.
Heart-kidney-stomochord complex (3)	Complex of three structures: a contractile pericardium (heart), that pressurizes blood in the heart sinus against a turgid rod of cells (stomochord), resulting in the filtration of blood waste through the thin glomerulus (kidney).	• Decay began with loss of external regularity as the pigmented glomerulus liquefied. • Decay proceeded inwards as the stomochord cell walls ruptured. • At times persisting into stage 3 as a discolored packet of tissue and blood.
Pre-oral ciliary organ (4)	A U-shaped band of cilia on the posterior proboscis that transports particles into the mouth (Gonzalez and Cameron 2009).	• Decayed rapidly and was always absent by the end of stage 2.
Nuchal skeleton (6)	A Y-shaped collagenous structure that underlies the proboscis stomochord anteriorly and bifurcates posteriorly into the dorsal to dorsolateral collar coelomic cavities.	• Remained pristine throughout the experiment, showing no signs of decay. • Connected to the gill bars by the basal lamina well into stage 3. • Detached from gill bars in stage 4.
Gill pores (7)	Paired, dorsolateral ectodermal pores that connect the gill slits and atrium to the external environment.	• Consistently the first characters to disappear with the breakdown of the surrounding ectoderm. • Consistently absent by stage 2.
Gill bars (8)	Serially paired dorsolateral collagenous bars that are inverted 'W' shape, and develop from the pharynx ectoderm.	• Remained pristine throughout the experiment, showing no signs of decay. • Adjacent gill bars became disarticulated in stage 4.
Trunk	The posterior vermiform soma or segment of the enteropneusts that includes the pharynx, esophagus, and intestine.	• Highly decay prone, but did not completely disintegrate until stage 4. • Intestinal ectoderm ruptured early. • Continued to fray and tear, until entire sections of the trunk were no longer contiguous. • Pharyngeal trunk less prone to decay and held together by the dorsal midline, basal lamina and paired collagenous gill bars.

Table 1. *Continued*

Character	Description	Pattern of decay
Trunk ventral midline (9)	Thin band of ectoderm overlying a longitudinal thickening of the ventral nerve plexus, or ventral trunk nerve cord. In *S. pusillus* and *B. occidentalis* there are well developed paired bands of longitudinal muscles paralleling either side of this midline.	• Rate of decay varied between individuals of *S. pusillus* and *B. occidentalis*. • Often persisting into stage 3, however local regions of the ventral midline would in some specimens disintegrate by stage 2. • Thick nerve plexus often last structure physically linking two sections of the digestive trunk.
Genital wings (10)	Of the three species examined, these paired dorso-lateral extensions of the trunk ectoderm are unique to *B. occidentalis* (a ptychoderid).	• Decay at a rate similar to other large features such as the proboscis and trunk. • Fraying and loss of structural rigidity in stage 2. • Total loss usually occurred by the end of stage 3.
Esophageal organ (11)	Shaped like opposing pillows and positioned between the pharynx and gut, it functions to squeeze excess water from the food cord. In *H. planktophilus*, it is a deep red-brown colour.	• Most decay resistant of the soft internal structures. • In *H. planktophilus*, remained identifiable until stage 3.
Trunk dorsal midline (12)	A thin band of ectoderm overlaying a longitudinal thickening of the dorsal nerve plexus or dorsal nerve cord.	• Rapid decay, usually lost in stage 2. • In *S. pusillus*, the paired ridges that parallel each side of the dorsal midline were quickly lost.
Hepatic sacs (13)	Blind finger-like extensions, or caeca, of the gut that project from the mid dorsal trunk of *B. occidentalis* (a ptychoderid). They increase the digestive and absorptive area of the gut.	• Decay at a rate similar to other large features such as the proboscis and trunk. • Lose most rigid definition and fray significantly by stage 2. • Total loss occurred by the end of stage 3.
Digestive tube (14)	The tubular endodermal gut, or intestine, begins after the esophageal organ and terminates at the anus.	• Rapid and early decay, lost by stage 3. • Ruptures were observed within 2 days, often accompanied by ruptures of the overlying ectoderm, spilling gut contents into external medium.

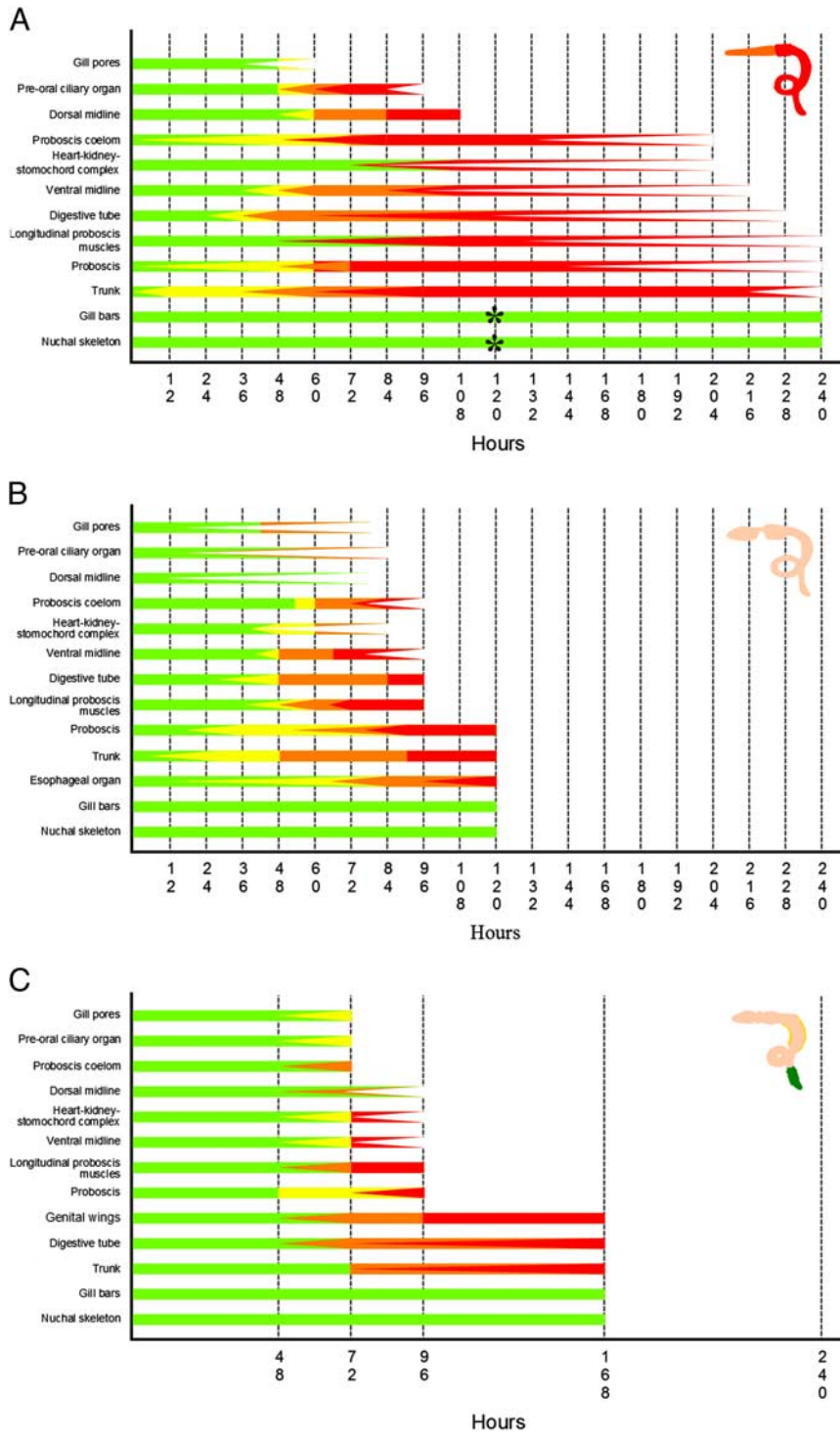

FIGURE 3. Sequence and rate of decay for three enteropneust species. A, *Saccoglossus pusillus*. B, *Harrimania planktophilus*. C, *Balanoglossus occidentalis*. Solid colors represent time intervals where the indicated level of decay was achieved for all trials. The tip of an arrow represents the first time interval where that level of decay was achieved. Green = level 1, yellow = level 2, orange = level 3, red = level 4, white = level 5 (absent). Asterisk indicates earliest point of gill bar/nuchal skeleton disarticulation.

https://doi.org/10.1017/pab.2015.11 Published online by Cambridge University Press

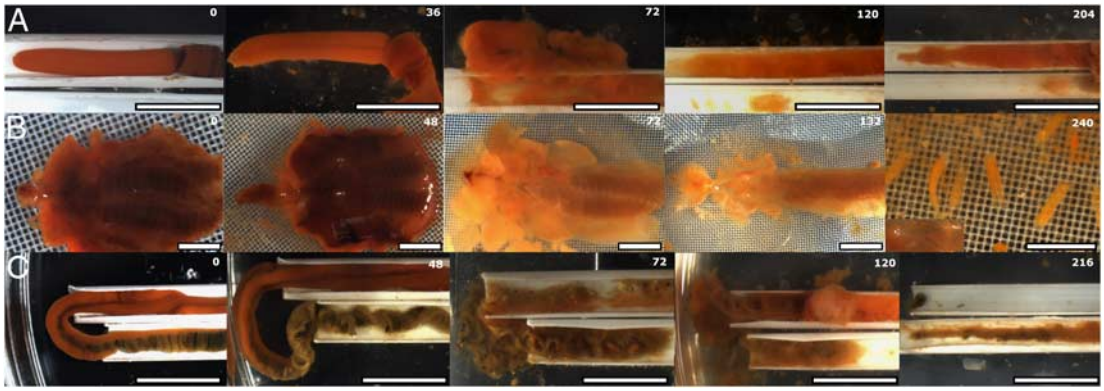

FIGURE 4. Sequence of decay of *Saccoglossus pusillus*. Rows from top to bottom: proboscis, pharyngeal area, trunk. Columns from left to right: pristine, decay stages 1–4. Scale bars in rows A and C, 1 cm, and in B, 1 mm. Time elapsed since euthanasia in hours in the top right of each cell.

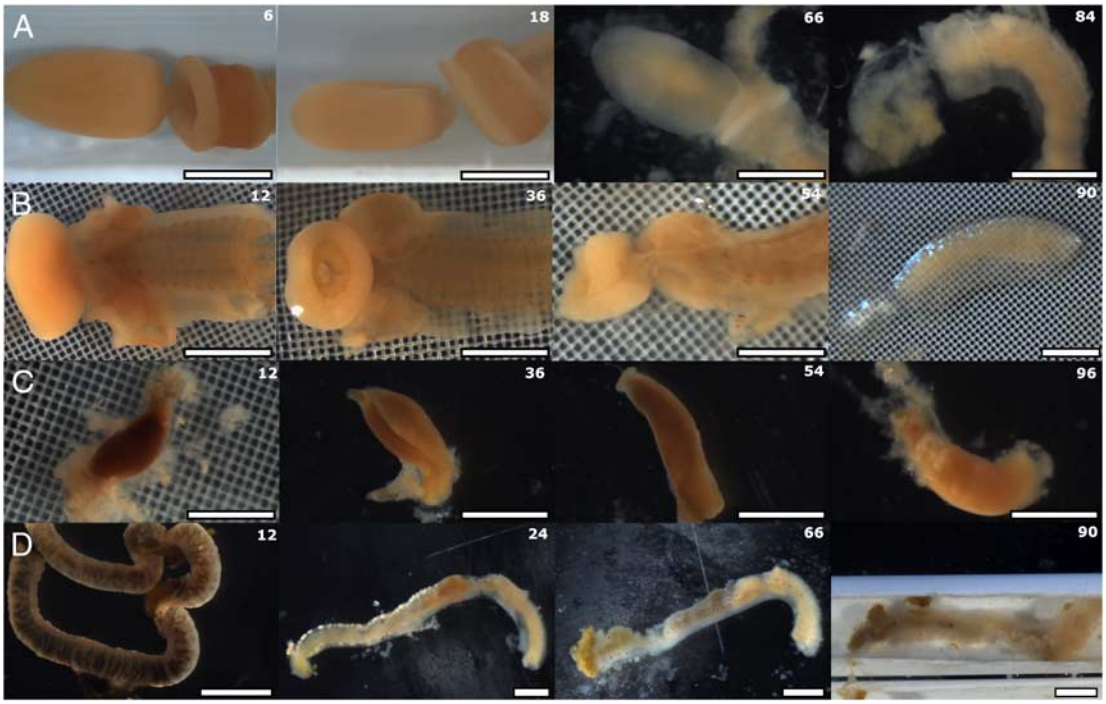

FIGURE 5. Sequence of decay of *Harrimania planktophilus*. Rows from top to bottom: proboscis, pharyngeal area, esophageal organ, trunk. Columns from left to right: decay stages 1–4. Scale bars, 1 mm. Time elapsed since euthanasia in hours in the top right of each cell.

were held together only along the ventral midline, where there is a thickening of the nerve plexus into a cord.

Stage 3 was characterized by the disintegration of all non-collagenous structures. The proboscis and general musculature of the trunk was completely without form. The straw maintained the overall shape of the enteropneust. The collagenous nuchal skeleton and gill bars were still contiguous and attached to each other by the basal lamina. The heart-kidney-stomochord complex was recognizable as a discolored or bloody patch near the anterior tip of the nuchal skeleton.

https://doi.org/10.1017/pab.2015.11 Published online by Cambridge University Press

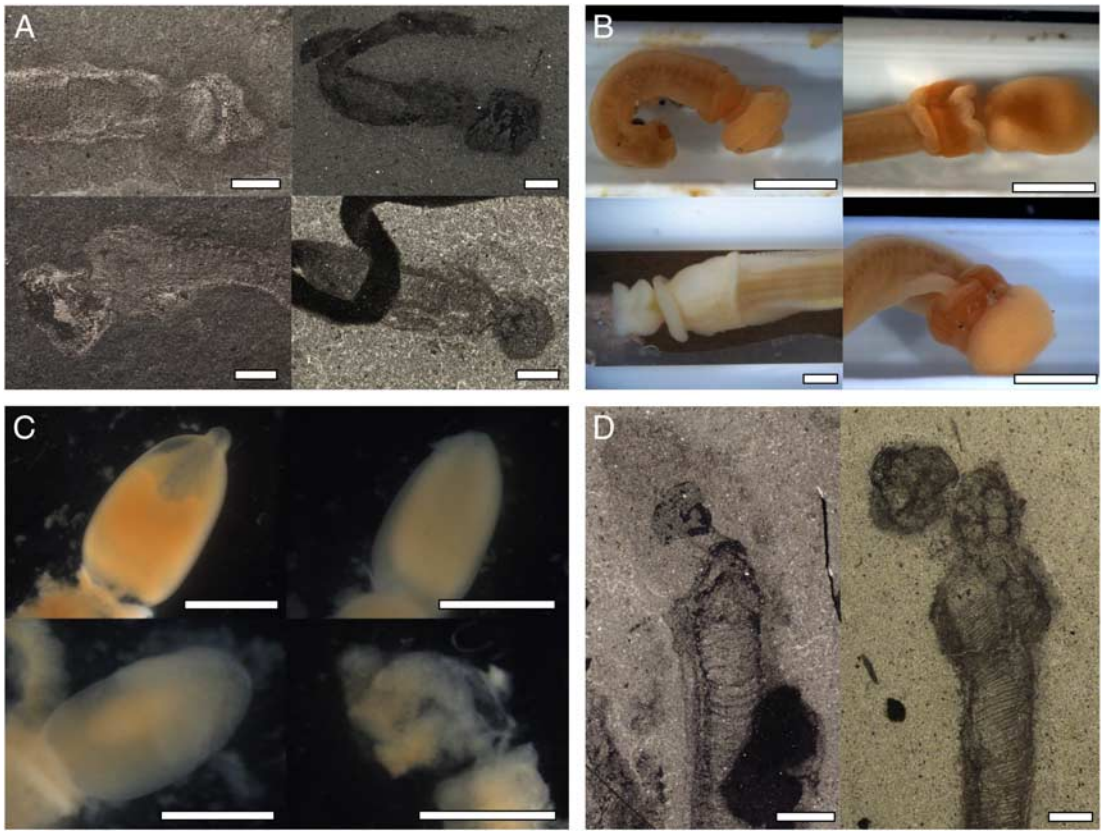

FIGURE 6. Proboscis morphology variations among *S. tenuis* specimens. A, The various shapes that a proboscis may take after death that differ from the traditional "acorn" type morphology. B, A direct comparison among these shapes and variation in proboscis preservation. C, Patchy local variation of muscle decay within the proboscis, compared with the patchy patterns of darkness/reflectivity in fossil taxa (D); A–C, clockwise from top left: ROM 62124, USNM 202841, ROM 62123, USNM 202797; D, left to right: USNM 202183, ROM 63129. Scale bars, 1 mm.

Stage 4 was the final stage of decay, in which all non collagenous structures are liquified. No internal structures maintains the specimen's shape. The nuchal skeleton and gill bars remained completely undamaged structurally, but were now freely disarticulated from what remained.

Fossil Comparisons

Proboscis.—There are two primary elements to consider when examining proboscis preservation in fossil enteropneusts in comparison with decay data: variation in general outline and preservation of internal organs.

Among *S. tenuis* and other tentatively described fossil enteropneusts, proboscis morphology is generally oblong and oval-shaped, as it is in their extant counterparts. However, some examples show squarer, less oblong, or irregular outlines (Fig. 6A). These variations in shape could be due to stress at the time of death and are reminiscent of what we observed in modern forms following euthanasia (Fig. 6B).

Potential internal features that have been identified within the proboscis include the heart-kidney-stomochord complex, the proboscis coelom, and the pre-oral ciliary organ (Caron et al. 2013). These characters, however, are highly prone to decay, particularly the pre-oral ciliary organ, which was consistently the second character to disappear, following the gill pores (Fig 3). The proboscis coelom also rapidly collapsed and began to show

https://doi.org/10.1017/pab.2015.11 Published online by Cambridge University Press

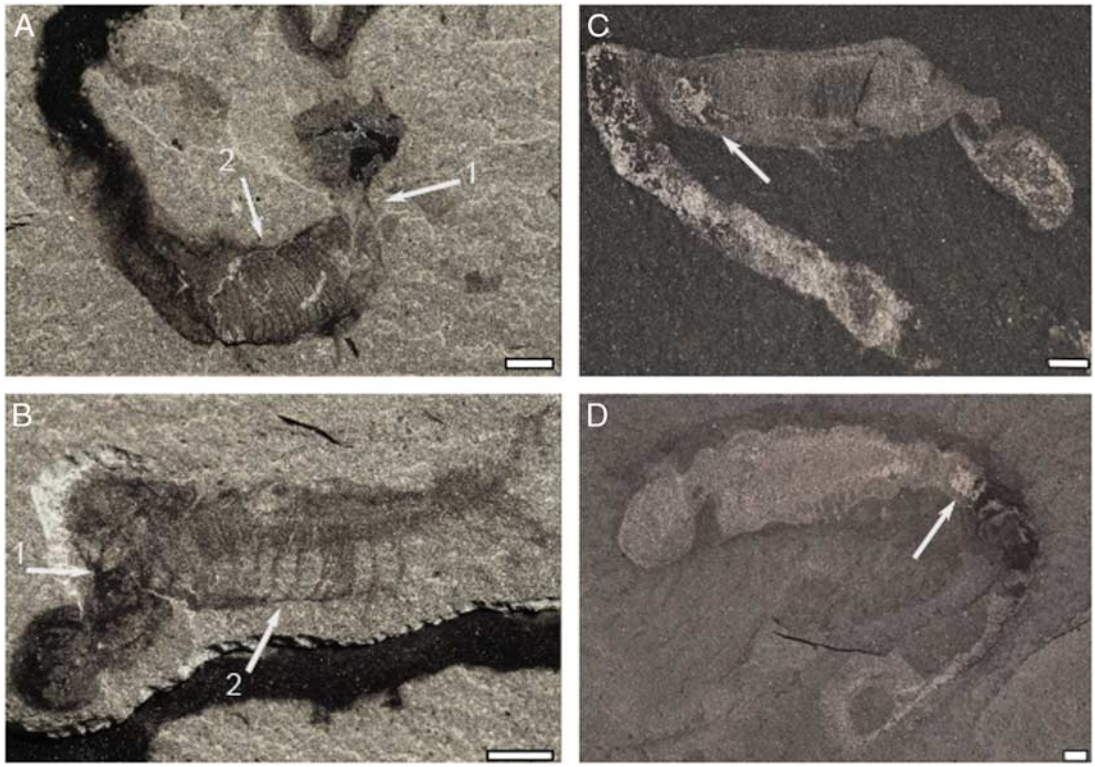

FIGURE 7. A, B, Preservation of clearly harrimaniid type nuchal skeletons (1) and gill bars (2). Scale bars = 1 mm. Orientation of preservation may result in variable presentations of the nuchal skeleton. A: the nuchal skeleton is preserved on a plane parallel to the fossil face (ROM 63128). B: the nuchal skeleton is preserved at a slight angle to the fossil face (USNM 202469). C and D: Preservation of the esophageal organ. The presence of a dark/reflective oblong patch at the end of the pharyngeal trunk after the gill bars corresponds to the anatomical position of the esophageal organ. The esophageal organ is the most decay-resistant soft character. C, USNM 202472. D, USNM 509806.

significant decay early in the decay sequence. The heart-kidney-stomochord complex was more resilient and persisted into stage 3 decay, but only as a tissue discoloration near the anterior tip of the nuchal skeleton. It was unlikely to have been fossilized in its characteristic ovular or spade shape, except in exceptionally well-preserved specimens.

Given that three of the suggested internal structures of the proboscis have relatively low fossilization potential, we propose instead that the features recognized in *S. tenuis* are the longitudinal proboscis muscles. In many specimens, darker zones are present within the proboscis, and the extent and shape of these zones is variable across specimens. This could be related to the extent of decay of the longitudinal proboscis muscles, as shown in extant forms (Fig. 6C,D).

Nuchal Skeleton and Gill Bars.—The nuchal skeleton and gill bars were the most decay-resistant features in the enteropneust anatomy (Fig. 3). Evidence of nuchal skeletons in *S. tenuis* includes their placement and size relative to the rest of the body and their wishbone-shaped morphology, which are consistent with the nuchal skeletons of extant enteropneusts (cf. Fig. 7A, and Fig. 2B). The skeletal arms are long and thin, pointing posteriorly towards the trunk, and join together to form a single, larger arm, pointing anteriorly.

Serial gill bars are the most common internal feature present in *S. tenuis*, and are often well preserved in comparison to the surrounding features. There was no evidence of structural damage to the gill bars in any of our decayed extant specimens. Likewise, no examples of *S. tenuis* present gill bars that appear to be

https://doi.org/10.1017/pab.2015.11 Published online by Cambridge University Press

fractured or otherwise damaged. The level of gill bar articulation in *S. tenuis* indicates the extent of pre-fossilization decay of the pharyngeal area: most specimens feature highly detailed and well-articulated gill bars that have maintained their positions and remain in close association with neighboring gill bars (Fig. 7A). Some are no longer parallel; that is, they exhibit a shifting of orientation relative to one another (Fig. 7B). The pharyngeal area of these specimens therefore indicates that decay had progressed to stage 3, the first point at which the basal lamina had degraded enough for the gill bars to move independently.

Resistance of the Esophageal Organ.—In *H. planktophilus*, the esophageal organ is the most decay-resistant of the soft internal organs (Fig. 3B). By late stage 2 and early stage 3, the esophageal organ was often relatively undamaged, whereas most surrounding tissues and the digestive tube had liquefied or begun to disintegrate. In *S. tenuis*, visually distinct patches have been identified directly posterior and ventral to the last set of gill bars in the pharynx. This position, the characteristic oval shape of this darkened or reflective region, and the relative decay resistance of the esophageal organ make it a good candidate for preservation (Fig. 7C,D).

Outline and External Features of Dead Specimens.—Across all three enteropneust species, the gill pores were the first character to disappear. Although it is not surprising that an exterior ectodermal feature did not last long in the decay process, it is significant because it implies that the absence of gill pores among fossil enteropneusts may be due to taphonomic effects and not necessarily a true phylogenetic absence. The clear visibility of internal features, such as the gill bars, also suggests the rapid decay of external tissues.

The genital wings of the ptychoderid *B. occidentalis* were also found to decay at a rate approximately equal to that of the rest of the trunk (Fig. 3B). This is to be expected, considering that they are extensions of the pharyngeal trunk.

The outlines of *S. tenuis* fossils, while clearly of vermiform shape, frequently exhibit signs of light decay, i.e., late stage 1 to stage 2. Moderately frayed or fuzzy borders are indicative of ectodermal decay, whereas more drastic and localized irregularities may be indicative of liquid seeping out of the body or fraying of the ectoderm.

The post-pharyngeal trunk often has the most irregular outline, consistent with both the naturally wrinkled shape of the trunk and the early onset of decay in the most posterior regions of the trunk (Figs. 3–5).

Discussion

Phylogeny.—A direct comparison of extant enteropneust morphology, the sequence of character decay, and fossil examples strongly supports the description of *S. tenuis* as a harrimaniid-like enteropneust that constructed pterobranch-like tubes (Caron et al. 2013). Like harrimaniid worms, *S. tenuis* has a nuchal skeleton but lacks gill bar synapticles, genital wings, hepatic sacs, and elaborations of the collar.

The collagenous nuchal skeleton and gill bars are by far the most decay-resistant structures in enteropneust anatomy (Fig. 3). These structures are well defined in *S. tenuis* and, as such, are crucial when inferring the phylogeny of the species. Among extant groups of enteropneusts, the shape of the nuchal skeleton of *S. tenuis* is most like that of the harrimaniids. It has thin skeletal cornua extending at least to the middle of the collar, in contrast to the thicker and blunter skeletal arms of ptychoderids and spengelids. The nuchal skeleton is nearly or entirely absent from the deep-sea torquaratorids (Osborn et al. 2012).

The gill bars of *S. tenuis* are well defined and clearly lack any evidence of collagenous synapticles bridging the primary and secondary gill bars. This represents a phylogenetic absence rather than a taphonomic loss because synapticules are materially identical to gill bars and nuchal skeleton, which are well preserved. The absence of gill bar synapticles is one of the features diagnostic of the family Harrimaniidae (and Torquaratoridae [Deland et al. 2010]), lending further support to this phylogenetic association.

There is also no evidence of ptychoderid-like hepatic sacs or genital wings in *S. tenuis*. The genital wings and hepatic sacs in extant enteropneusts decay at the same rate as the

https://doi.org/10.1017/pab.2015.11 Published online by Cambridge University Press

ectoderm and other superficial features. We would therefore expect evidence of one or both of these structures among the many examples of *S. tenuis* with well-preserved external outlines. Genital wings have been found in the Jurassic enteropneust *Mesobalanoglossus buergeri*, further supporting their absence rather than a taphonomic loss in *S. tenuis* (Bechly and Frickhinger 1999).

An argument has been made for the association of *S. tenuis* with the deep-sea enteropneust clade Torquaratoridae (Halanych et al. 2013; Cannon et al. 2013), but it is based solely on the resemblance between mucus tubes that are constructed by some torquaratorids, and that have been noted to persist after being evacuated by the enteropneust, and those of *S. tenuis*. This argument is weak because torquaratorids and *S. tenuis* are morphologically unalike, similarities between the mucus tubes and fossilized burrows are superficial, and torquaratorids live in the deep sea, unlike the relatively shallow-water Burgess Shale shelf fauna.

The most visually striking difference between the torquaratorids and *S. tenuis* is collar morphology. The unadorned collar region of *S. tenuis* stands in contrast to the more complex and often "appendaged" collar region of most torquaratorids. Although we have not observed the decay of any deep-sea acorn worms, there is no reason to believe that their collar appendages differ significantly enough in composition from the collar itself to have caused their selective absence from the fossil record. Rather, hypothetical fossil torquaratorids should present some range of collar appendage preservation corresponding to the preservation level of other, more ubiquitous, enteropneust characters.

The nuchal skeleton of *S. tenuis* also distances it from the Torquaratoridae. The torquaratorids generally lack nuchal skeletons and, when they are present, they are reduced to a medial plate. The possibility that *S. tenuis* represents the direct ancestor leading to the torquaratorid line, and that the nuchal skeleton was subsequently lost, is also unlikely. This positioning would place *S. tenuis* in a close relationship to the ptychoderids, which we have already rejected on the basis of ample morphological differences between *S. tenuis* and the Ptychoderidae.

The visual similarity of the tubes is most likely misleading. In general, perhaps without exception, enteropneusts secrete copious amounts of mucus. The construction of mucus tubes has been observed in many enteropneusts and is not an exclusive feature of the torquarotorids (Urata and Yamaguchi 2004; Gonzalez and Cameron 2009). Therefore, *S. tenuis* cannot be placed with the torquarotorids exclusively on the basis of these secretions. Further, tube breakages, when present in *S. tenuis*, are typically abrupt terminations between the displaced fragments, indicating a rigid structure (Fig. 8), like the tubes of pterobranch hemichordates (Caron et al. 2013). The tubes constructed by torquaratorids appear to be mucus-based and have been inferred to contain proteinaceous elements that contribute to their longevity. Pliable tubes such as these seem more likely to tear and pull apart raggedly rather than break cleanly when exposed to similar external forces, demonstrating a fundamental difference in composition and structure between the tubes constructed by *S. tenuis* and torquaratorids.

The decay rate of the torquaratorid tubes is also difficult to reconcile with the fossil record because they appear to have lost most of their obvious structure within 24 hours, and to have disintegrated between 48 and 60 hours post-evacuation. This rapid decay is comparable to that of decay-prone organs, such as the gill pores and pre-oral ciliary organ, that disappear in stage 2 (and which we have found no conclusive evidence of in any specimen of *S. tenuis*). Unlike mucus secretions, the tubes of *S. tenuis* tubes consistently preserve high levels of detail, with relatively little decay (Fig. 8), further emphasizing a compositional difference between the mucus tubes of torquaratorids and the indeterminate fossil tubes. The rapid rate of mucus decomposition likely explains the total absence of fossilized mucus among Cambrian biota.

The combination of a rigid tube structure and the overwhelming similarity between *S. tenuis* and the harrimaniids suggests that tube dwelling is an ancestral trait for the hemichordates and that it was lost leading up to the enteropneusts. *S. tenuis* represents a stem-enteropneust possessing the acorn worm apomorphic characters, gill bars, and nuchal skeleton (hypothesis 3 in Fig. 1).

https://doi.org/10.1017/pab.2015.11 Published online by Cambridge University Press

FIGURE 8. Tube structures in *S. tenuis* show high degrees of preservation with clearly defined edges, in contrast with the rapidly disintegrating mucus tubes of extant torquaratorids (clockwise from top left: ROM 62129, ROM 63126, USNM 202097, ROM 63127). Scale bars, 1 cm. Breakages terminate more abruptly than would be expected for a mucus-based structure.

Incongruities.—There are two primary incongruities between the decay data and fossils of *S. tenuis*. The first is the preservation of characters inconsistent with the stages of decay observed in our experiment (Fig. 9). Examples A and B in Figure 9 present partial gill bar disarticulation but relatively little decay of the proboscis and digestive trunk, i.e., the area posterior to the pharyngeal trunk. The state of the gill bars by itself might suggest that the fossils reached late stage 3 to stage 4 prior to diagenesis, but based on the proboscis and post-pharyngeal trunk, the fossil appears to have begun preservation at stage 2. One possible explanation is that, prior to or during a burial event, the pharyngeal areas of these specimens were damaged. Lesions breaking through the ectoderm could have accelerated the decay of the surrounding area, leading to early disassociation of the gill bars relative to the expected sequence of decay.

The second incongruity is the unusual positioning of otherwise well-preserved structures. Some specimens show nuchal skeleton-shaped characters that are not perfectly congruous with their expected position. However, these structures are never far from the "neck" of the fossil, where the proboscis connects to the trunk and where the nuchal skeleton is located. These displacements take the form of slight shifts or rotations relative to their expected positions (Fig. 6A,B). These topographic differences can be explained by considering the sequence of enteropneust decay. At stage 4, the collagenous nuchal skeleton and gill bars are the only remaining undamaged characters. Soft tissue has lost all structural integrity and elasticity, and connective tissue, including muscle, has disintegrated or liquefied. By the end of this stage, the nuchal skeleton and gill bars are completely disarticulated from any connecting structures and can freely move through the enteropneust remains. It therefore seems likely that *S. tenuis* specimens displaying the aforementioned nuchal skeleton displacement, while still providing evidence of an

https://doi.org/10.1017/pab.2015.11 Published online by Cambridge University Press

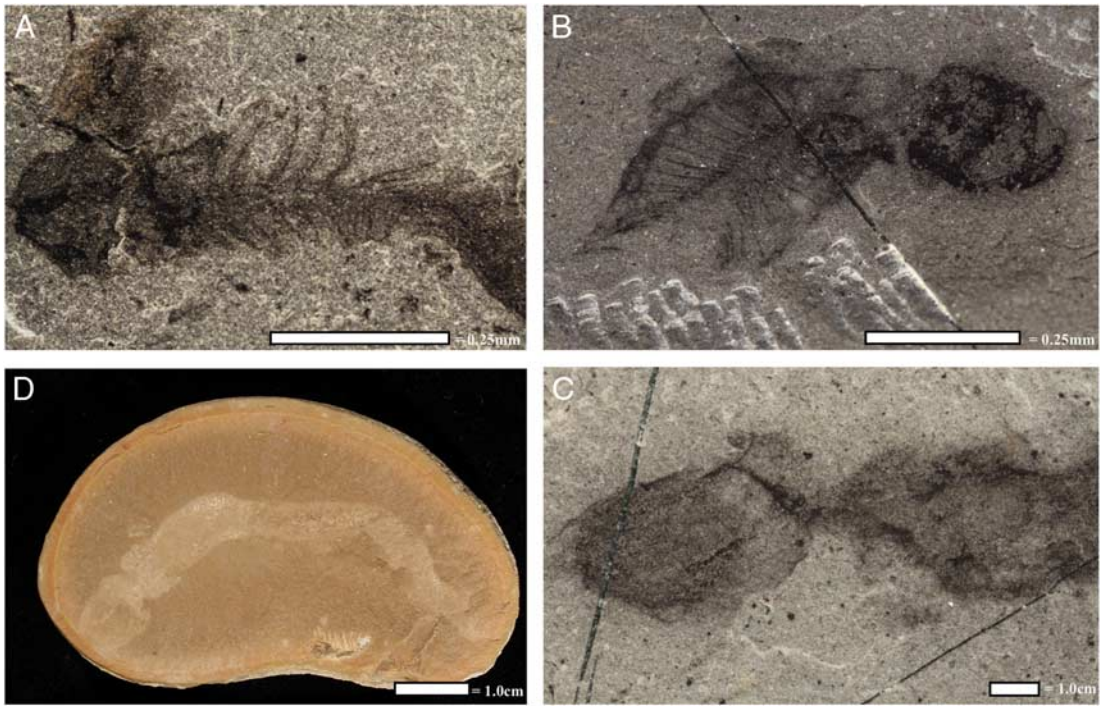

FIGURE 9. Incongruities between decay data and the fossil record (clockwise from top left: ROM 63124, USNM 202780, ROM 63125). A, B, High degrees of pharyngeal decay relative to the proboscis and digestive trunk, an inversion of what would be expected. C, A nuchal skeleton structure, rotated 180° from its expected orientation. There is no evidence that the proboscis has been disturbed; thus the external factors that resulted in this orientation are unclear. D, The Mazon Creek taxon *Mazoglossus ramsdelli*; although the tripartite body outline of an enteropneust is unequivocal, there is no discernible preservation of internal features.

undamaged nuchal skeleton shaped structure, died and proceeded to degrade to late stage 3, when they were then buried and subsequently fossilized. These individuals would represent the most advanced state of decay that could reliably produce fossils recognizable as *S. tenuis*. A more extreme example of this phenomenon is the 180º rotation of a nuchal skeleton-like structure in Figure 9C. There is no other evidence of significant postmortem disturbance of this specimen, and therefore the drastic repositioning of the nuchal skeleton defies explanation based on decay data.

Although significant inconsistencies between character preservation and the observed stages of decay are rare in *S. tenuis*, the Mazon Creek enteropneust taxon *Mazoglossus ramsdelli* differs fundamentally in preservation (Fig. 9D). *M. ramsdelli* clearly displays the tripartite enteropneust body plan of proboscis, collar, and trunk. Fossil outlines present varying degrees of clarity and regularity, representing varying degrees of pre-diagenetic decay. However, no specimens display any observable internal characteristics. This is a marked departure from the preservation style of *S. tenuis*, of which there are abundant examples of gill bar and nuchal skeleton preservation, as well as consistent patterns of soft-tissue preservation.

These inconsistencies between fossil presentation and the decay data do not invalidate the usefulness of decay experiments when considering taphonomy. Instead, they emphasize that, rather than being completely diagnostic of the processes that lead to fossilization, decay experiments conducted in non-actualistic conditions provide benchmarks against which descriptions of fossil taxa can be measured. Deviations from these benchmarks can themselves be informative as inferences can be made regarding the nature of fossilization conditions, which may differ from observed laboratory decay sequences.

https://doi.org/10.1017/pab.2015.11 Published online by Cambridge University Press

Burgess Shale Taphonomy.—Burgess Shale-type preservation begins with the rapid entombment of organisms by mud-silt flows (Allison and Brett 1995; Gabbott et al. 2008). The speed of these depositional events, in combination with the precipitation of carbonate cements acting as a permeability barrier at the sediment-water interface, quickly limited the availability of oxidants required for microbial decay, and thus impeded decomposition (Gaines et al. 2012). Most preserved features remain as flattened (often two-dimensional) carbonaceous compressions, although preservation of some features may have involved pyritization and phosphatization (Butterfield 2002; Gabbott et al. 2004; Gaines et al. 2012).

Although there is some debate regarding the extent to which Burgess Shale organisms were transported prior to fossilization (Gabbott et al. 2008), biostratinomic evidence shows that the amount of transport must have been limited and most fossils were preserved close to their living habitat (Caron and Jackson 2006).

The goal of our experiment was to quantify the rate of morphological decay in enteropneusts regardless of the peculiar taphonomic conditions that might have been present at the Burgess Shale. To this end, we did not investigate the role of water chemistry or sediment type (e.g., pore size, chemical composition), or attempt to describe the chemical pathways that may have led to exceptional preservation. However, our observations of the unimpeded sequence and rate of decay of morphological characters of the Enteropneusta provide the framework for interpreting the fossil anatomy of *S. tenuis* and of future hemichordate fossils from other fossil deposits, as well as for making broader inferences regarding the potential paleoenvironmental conditions of the Cambrian.

Comparing the quality of preservation of *S. tenuis* with the sequence and rate of decay in extant enteropneusts can inform estimates of the speed of fossilization in the Burgess Shale. Enteropneusts are entirely soft-bodied organisms, and can progress from death to almost complete disintegration within the span of 5 to 8 days at 17°C. This short time frame and the high quality of soft-tissue preservation displayed by many Burgess Shale fossils suggest that mineralization must have occurred soon after death, and/or that decay must have been halted or significantly slowed. The rapid decay rates of enteropneust tissues in this study therefore lend support to previous work that showed that Burgess Shale-type preservation is most likely the result of suppression of natural decay processes (Gaines et al. 2008, 2012).

Another feature of taphonomy revealed by the speed and sequence of enteropneust decay is the extent of pre- versus post-burial decay present in *S. tenuis* specimens. Very few specimens are likely to have undergone significant pre-burial decay, because after stage 2, any directional, external force would have been capable of radically shifting the topography of the remains, and liquefying tissues would have leaked out and away from the body. The well-articulated nature of most of these fossils indicates that organisms were likely buried before significant decay had occurred, because *S. tenuis* corpses are held together in a manner similar to that seen in the extant enteropneusts held in place in our experiments using a plastic trough.

Our observations also support the theory that most specimens presenting high-quality preservation likely did not undergo significant transport and experienced minimal disturbance post-burial (Caron and Jackson 2006). The anatomy of enteropneusts is extremely fragile; it is not uncommon for them to suffer trunk damage or tearing of the tissues surrounding the nuchal skeleton during extraction and transport. Similarly, post-burial disturbance would likely result in significant shifts in topology, contingent upon the level of decay at the point of disturbance.

There is, however, some evidence for movement when considering that *S. tenuis* specimens are found both as isolated fossils and in assemblages. Isolated fossils exhibit a much higher degree of resolution of fine details and tend to be more-articulated specimens than specimens preserved in assemblages. In contrast, assemblages of *S. tenuis* often display particularly poor resolution; large collections of bodies crisscross and lie on top of each other (Fig. 10 left). The scattered orientation of the various specimens may be indicative of tumbling during a depositional event. In these cases of significant transport, there is greater evidence of damage to

https://doi.org/10.1017/pab.2015.11 Published online by Cambridge University Press

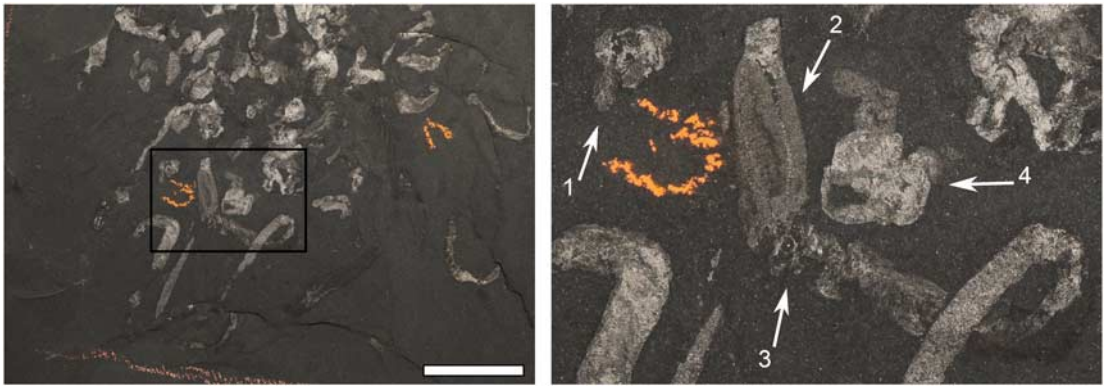

FIGURE 10. Left, Assemblages of *S. tenuis* may be indicative of a depositional event gathering several specimens together (USNM 202603). Scale bar, 1 cm. Right, close up of framed area. Such assemblages typically display signs of damage related to movement (USNM 202603). 1, Likely a detached proboscis lost during motion. 2, A comparatively well-preserved pharyngeal area displaying high gill bar clarity. 3, Significant post-pharyngeal damage to the trunk. 4, An unidentifiable, disarticulated tissue mass.

specimens, including detachment of the proboscis and possible tearing of muscle tissues (Fig. 10 right).

Finally, an important point is that we did not see any trend in morphological character loss consistent with the concept of "stemward slippage." Stemward slippage is the proposed underlying bias toward erroneously interpreting fossil taxa as basal due to the preferential loss of synapomorphic characters before plesiomorphic characters during decay (Sansom et al. 2010a). Among enteropneusts, stemward slippage was not observed. Phylogenetically informative characters may be either decay-susceptible or decay-resistant. Derived family-specific characters such as the genital wings and hepatic sacs are prone to decay, but no more so than the ectoderm and other external features of the class Enteropneusta. On the other hand, the nuchal skeleton, an autapomorphy of the Enteropneusta, and the gill bars, a plesiomorphic character of the deuterostomes, are the most decay-resistant structures in enteropneust anatomy. Resistance to decay is more appropriately thought of as a consequence of the size and composition of a morphological feature.

Conclusions

Although decay data do not completely explain all patterns of preservation observed in fossilized enteropneusts, we argue that the true strength of decay data is that a comprehensive understanding of decay allows us to produce a laboratory benchmark against which we can evaluate the degree to which decay may have proceeded in fossil forms before the process of preservation stopped it.

Our study of the decay of extant enteropneusts reveals that the sequence of morphological character decay is consistent across the three species studied; these species represent a disparate taxonomic sampling of the group. However, despite this consistency, we did not observe any meaningful bias favoring loss of synapomorphic characters over plesiomorphic characters. We conclude, therefore, that the stemward slippage hypothesis is not affecting our description and phylogenetic placement of *S. tenuis*.

Using decay data as a benchmark when analyzing the Cambrian fossil enteropneust *S. tenuis*, we have confidently identified all major structural features and conclude that it is most like members of the family Harrimaniidae. This conclusion reinforces the view (Caron et al. 2013) that the morphologically simple harrimaniid body plan has been conserved over 500 Myr with little observed change.

Acknowledgments

We thank P. Fenton for assistance in the collections and the director and staff of the

https://doi.org/10.1017/pab.2015.11 Published online by Cambridge University Press

Bamfield Marine Sciences Centre. We also thank S. Darroch and J. D. Schiffbauer for their constructive comments which substantially improved the manuscript. The decay study was supported by C. B. Cameron's Discovery Grant from the Natural Sciences and Engineering Research Council of Canada (NSERC). K. Nanglu's doctoral research is supported by fellowships from the University of Toronto (Department of Ecology and Evolutionary Biology) and J.-B. Caron's NSERC Discovery Grant (#341944). This is Royal Ontario Museum Burgess Shale project number 61.

Literature Cited

Alessandrello, A., G. Bracchi, and B. Riou. 2004. Polychaete, sipunculan and enteropneust worms from the lower Callovian (Middle Jurassic) of La Voulte-sur-Rhône (Ardèche, France). Atti della Società italiana di Scienze naturali e del Museo Civico di Storia naturale di Milano 32:3–14.

Allison, P. A. 1986. Soft-bodied animals in the fossil record: the role of decay in fragmentation during transport. Geology 14:979–981.

——. 1988. The role of anoxia in the decay and mineralization of proteinaceous macro-fossils. Paleobiology 14:139–154.

Allison, P. A., and C. E. Brett. 1995. In situ benthos and paleo-oxygenation in the Middle Cambrian Burgess Shale, British Columbia, Canada. Geology 23:1079–1082.

Arduini, P., G. Pinna, and G. Teruzzi. 1981. *Megaderaion sinemuriense* ng. n.sp, a new fossil enteropneust of the Sinemurian of Osteno in Lombardy. Atti della Societa Italiana di Scienze Naturali e dei Museo Civico di Storia Naturalie di Milano 122:104–108.

Bechly, G., and K. A. Frickhinger. 1999. The fossils of Solnhofen 2. Goldschneck, Korb, Germany.

Briggs, D. E. G., and A. J. Kear. 1993a. Decay of *Branchiostoma*: implications for soft-tissue preservation in conodonts and other primitive chordates. Lethaia 26:275–287.

——. 1993b. Decay and preservation of polychaetes—taphonomic thresholds in soft-bodied organisms. Paleobiology 19:107–135.

——. 1994. Decay and mineralization of shrimps. Palaios 9: 431–456.

Briggs, D. E. G., A. J. Kear, M. Baas, J. W. Leeuw, and S. Rigby. 1995. Decay and composition of the hemichordate *Rhabdopleura*: implications for the taphonomy of graptolites. Lethaia 28: 15–23.

Butterfield, N. J. 2002. *Leanchoilia* guts and the interpretation of three-dimensional structures in Burgess Shale-type fossils. Paleobiology 28:155–171.

Cameron, C. B. 2002. Particle retention and flow in the pharynx of the enteropneust worm *Harrimania planktophilus*: the filter feeding pharynx may have evolved prior to the chordates. Biological Bulletin 202:192–200.

——. 2005. A phylogeny of the hemichordates based on morphological characters. Canadian Journal of Zoology 83:196–215.

Cameron, C. B., B. J. Swalla, and J. R. Garey. 2000. Evolution of the chordate body plan: new insights from phylogenetic analysis of deuterostome phyla. Proceedings of the National Academy of Sciences USA 97:4469–4474.

Cannon, J. T., B. J. Swalla, and K. M. Halanych. 2013. Hemichordate molecular phylogeny reveals a novel cold-water clade of harrimaniid acorn worms. Biological Bulletin 225:194–204.

Caron, J. B., and D. A. Jackson. 2006. Taphonomy of the Greater Phyllopod Bed community, Burgess Shale. Palaios 21:451–465.

Caron, J. B., S. Conway Morris, and C. B. Cameron. 2013. Tubicolous enteropneusts from the Cambrian period. Nature 495: 503–506.

Casenove, D., T. Oji, and T. Goto. 2011. Experimental taphonomy of benthic chaetognaths: implications for the decay process of Paleozoic chaetognath fossils. Paleontological Research 15: 146–153.

Chen, J. Y., J. Dzik, G. D. Edgecombe, L. Ramsköld, and G. Q. Zhou. 1995. A possible Ealy Cambrian chordate. Nature 377:720–722.

Chen, A., and D. Huang. 2008. Gill rays of the primitive vertebrate *Yunnanozoon* from Early Cambrian: a first record. Frontiers of Biology in China 3:241–244.

Conway Morris, S.. 2009. The Burgess Shale animal *Oesia* is not a chaetognath: a reply to Szaniawski. Acta Palaeontologica Polonica 54:175–179.

Conway Morris, S., and J. B. Caron. 2012. *Pikaia gracilens* Walcott, a stem-group chordate from the Middle Cambrian of British Columbia. Biological Reviews 87:480–512.

Darroch, S. A. F., M. Laflamme, J. D. Schiffbauer, and D. E. G. Briggs. 2012. Experimental formation of a microbial death mask. Palaios 27:293–303.

Deland, C., C. B. Cameron, T. H. Bullock, K. P. Rao, and W. E. Ritter. 2010. A taxonomic revision of the family Harrimaniidae (Hemichordata: Enteropneusta) with descriptions of seven species from the Eastern Pacific. Zootaxa 2408:1–30.

Donoghue, P. C. J., and M. Purnell. 2009. Distinguishing heat from light in debate over controversial fossils. BioEssays 31: 178–189.

Gabbott, S. E., H. Xian-guang, M. J. Norry, and D. J. Siveter. 2004. Preservation of Early Cambrian animals of the Chengjiang biota. Geology 32:901–904.

Gabbot, S. E., J. Zalasiewicz, and D. Collins. 2008. Sedimentation of the Phyllopod Bed within the Cambrian Burgess Shale Formation of British Columbia. Journal of the Geologic Society 165: 307–318.

Gaines, R. R., D. E. G. Briggs, and Z. Yuanlong. 2008. Cambrian Burgess Shale-type deposits share a common mode of fossilization. Geology 36:755–788.

Gaines, R. R., E. U. Hammarlund, X. Hou, C. Qi, S. E. Gabbott, Y. Zhao, J. Peng, and D. E. Canfield. 2012. Mechanism for Burgess Shale-type preservation. PNAS 109:5180–5184.

Gonzalez, P., and C. B. Cameron. 2009. The gill slits and pre-oral ciliary organ of *Protoglossus* (Hemichordata: Enteropneusta) are filter feeding structures. Biological Journal of the Linnean Society 98:896–906.

Halanych, K. M., J. T. Cannon, A. R. Mahon, B. J. Swalla, and C. R. Smith. 2013. Modern Antarctic acorn worms form tubes. Nature Communications 4, doi: 10.1038/ncomms3738.

Maletz, J. 2014. Hemichordata (Pterobranchia, Enteropneusta) and the fossil record. Palaeogeography, Palaeclimatology, Palaeoecology 398:16–27.

Mitchell, C. E., J. M. Melchin, C. B. Cameron, and J. Maletz. 2013. Phylogeny of the tube-building Hemichordata reveals that *Rhabdopleura* is an extant graptolite. Lethaia 46:34–56.

Osborn, K. J., L. A. Kuhnz, I. G. Priede, M. Urata, A. V. Gebruk, and N. D. Holland. 2012. Diversification of acorn worms (Hemichordata, Enteropneusta) revealed in the deep sea. Proceedings of the Royal Society of London B 279:1646–1654.

Sansom, R. S., and M. A. Wills. 2013. Fossilization causes organisms to appear erroneously primitive by distorting evolutionary trees. Scientific Reports 3:2545.

Sansom, R. S., S. E. Gabbott, and M. A. Purnell. 2010a. Non-random decay of chordate characters causes bias in fossil interpretation. Nature 463:797–800.

——. 2010b. Decay of vertebrate characters in hagfish and lamprey (Cyclostomata) and the implications for the vertebrate fossil record. Proceedings of the Royal Society of London B 278:1150–1157.

——. 2013. Atlas of vertebrate decay: a visual and taphonomic guide to fossil interpretation. Palaeontology 56:457–474.

Shabica, C. W., and A. A. Hay. 1997. Richardson's guide to the fossil fauna of Mazon Creek. Northeastern Illinois University, Chicago.

Shu, D., X. Zhang, and L. Chen. 1996. Reinterpretation of *Yunnanozoon* as the earliest known hemichordate. Nature 380: 428–430.

Swalla, B. J., and A. B. Smith. 2008. Deciphering deuterostome phylogeny: molecular, morphological and palaeontological perspectives. Philosophical Transactions of the Royal Society B of London 363:1557–1568.

Szaniawski, H. 2005. Cambrian chaetognaths recognized in Burgess Shale fossils. Acta Palaeontologica Polonica 50:1–8.

——. 2009. Fossil chaetognaths from the Burgess Shale: a reply to Conway Morris. Acta Palaeontologica Polonica 54: 361–364.

Urata, M., and M. Yamaguchi. 2004. The development of the enteropneust hemichordate *Balanoglossus misakiensis* Kuwano. Zoological Science 21:533–540.

Wilson, L. A., and N. J. Butterfield. 2013. Sediment effects on preservation of Burgess Shale-type compression fossils. Palaios 29:145–153.

https://doi.org/10.1017/pab.2015.11 Published online by Cambridge University Press